ErAs enhanced active photonic THz components

M. Méndez Aller
Dept. of Electrical Engineering and Information Technology
TU Darmstadt
Darmstadt, Germany
aller@imp.tu-darmstadt.de

U. Nandi
Dept. of Electrical Engineering and Information Technology
TU Darmstadt
Darmstadt, Germany
Nandi@imp.tu-darmstadt.de

H. Lu
College of Engineering and Applied Sciences
University of Nanjing
Nanjing, China
hlu@nju.edu.cn

J.C. Norman
Materials Department,
University of California, Santa Barbara
Santa Barbara, USA
jnorman@umail.ucsb.edu

A.C. Gossard
Materials Department,
University of California, Santa Barbara
Santa Barbara, USA
gossard@engineering.ucsb.edu

S. Preu
Dept. of Electrical Engineering and Information Technology
TU Darmstadt
Darmstadt, Germany
preu@imp.tu-darmstadt.de

***Abstract*—We present active, telecom-wavelength compatible THz components with enhanced performance by introducing ErAs precipitates. First, we review how an ErAs monolayer in between p-i-n diodes enables serial connection of these diodes, reducing the total capacitance and thus decoupling the existing trade-off between RC- and transit time roll-off. In the second part of the paper, latest results with ErAs:In(Al)GaAs photoconductive devices are shown. Continous-wave (CW) receivers show an almost flat frequency response up to 0.5 THz with a noise equivalent power (NEP) of 20±10 fW/Hz. Under pulsed operation, we achieved 40 dB dynamic range at 4.1 THz with a system only using ErAs:In(Al)GaAs photoconductors as source and receiver.**

***Index Terms*—Terahertz materials, Terahertz radiation, photomixer, photoconductor**

I. Introduction

Photomixers operated at 1550 nm are important devices for both spectroscopic applications [1], [2] and communication technology [3]–[5]. Under continuous-wave (CW) operation, photomixers absorb an optical beat note between two continuous-wave (CW) lasers that run with a difference frequency of the desired THz signal. They generate a photocurrent containing the beat frequency and are typically attached to an on-chip antenna in order to radiate the THz signal. For pulsed operation, a single pulsed laser (typ. $<$ 100 fs), covering several THz bandwidth acts like an optical hammer stroke, generating a photocurrent with a large bandwidth that is, similar to CW, radiated by an antenna. For spectroscopy, photomixing systems offer extreme bandwidths in the range of several THz for both pulsed and CW operation. For communication applications, a fast photodiode is required to convert the data encoded on an optical carrier to an electrical signal for further data processing. For mm-wave or THz wireless communication applications, photomixers are further employed to generate the WiFi signal. Many efforts are currently undertaken to generate high bit rate communication systems that operate at carrier frequencies beyond 100 GHz, exploring yet unused telecom bands [6], [7]. A key requirement for such applications are efficient photonic sources and receivers. In this paper we address two photonic concepts for THz generation and detection that utilize ErAs precipitates in order to enhance the materials properties tailored to THz performance.

II. The n-i-pn-i-p superlattice photomixer

Typical p-i-n diode based photomixer concepts, such as uni travelling carrier diodes, have to trade-off above a few 100 GHz between transit-time and RC performance: while the transit time roll-off 3dB frequency (f_{tr}^{3dB}) scales with the inverse of the transport layer length (l_i^{-1}), the RC roll-off 3 dB frequency (f_{RC}^{3dB}), however, scales with the transport layer length, l_i. The transit time can be reduced by using quasi-ballistic transport [8], which allows average velocities up to 5×10^7 cm/s for InGaAs. This implies at best a maximum transport layer length of 250 nm for a f_{tr}^{3dB} of 1 THz. At the same time, transport layers longer than 900 nm for diodes with a cross-section in the range of 15-20 μm^2 are required to push the f_{RC}^{3dB} frequency towards 1 THz for a typical antenna radiation resistance of 70 Ω. Lower diode cross sections allow for shifting the RC 3 dB frequency to higher values, however,

978-1-5386-1221-7/18/$31.00 ©2018 IEEE

also limit the maximum optical power to be used for the device. The n-i-pn-i-p superlattice concept overcomes this trade-off by stacking a number of N p-i-n diodes and reducing the total capacitance by $C_{SL} = C_{pin}/N$ without affecting f_{tr}^{3dB}. An additional np junction forms between subsequent periods. This np junction has to feature a very low serial resistance for preventing accumulation of photogenerated carriers that would result in a flat band condition without any further functionality. These recombination diodes are achieved by introducing 1.2-1.7 monolayers (ML) of semi-metallic ErAs between the highly doped n and p layers [9]. Further details on InGaAs n-i-pn-i-p superlattice photomixers are found in [10]. For highest THz power levels in the range of 1 μW at 1 THz, these devices are operated with several 100 mW of laser power [10]. Such power levels are generally too high for communication applications where power levels below 100 mW are used. Fig. 1 shows the THz power emitted by a three period n-i-pn-i-p superlattice photomixer at an optical power of 95 mW, resulting in a photocurrent of 4 mA. At such low photocurrent, the THz power is about 1 μW at 0.5 THz, corrected for the reflection of the silicon lens. The device is illuminated from the top, resulting in a total absorption of only about 15% of the laser power. Waveguide-integration [3], [11] would be a solution to increase the photocurrent by absorbing the laser signal along the structure, therefore reducing the required power level by a factor of 5-7, depending on the waveguide coupling losses.

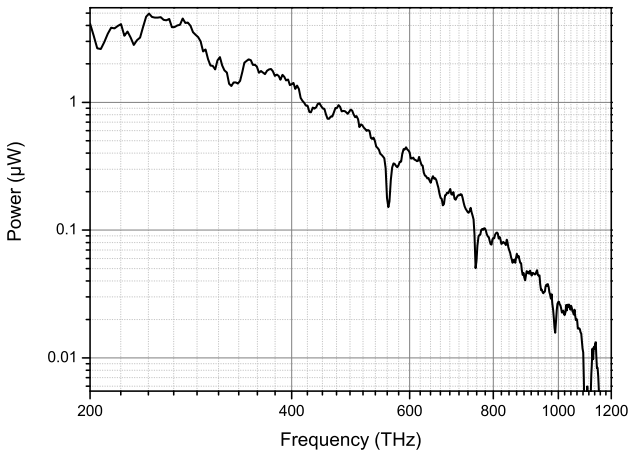

Fig. 1. Emitted power of a three period n-i-pn-i-p superlattice photomixer.

III. ErAs:InGaAs photoconductive receivers, continuous-wave operation

CW systems employing photoconductive receivers allow for homodyne detection with excelling low noise equivalent power at room temperature. For detection, these devices mix an incident laser beam, $P_L(t) = \cos\omega t$ that was used at the source side for THz generation with the received THz field, $E_{THz}(t) = \cos(\omega t + \varphi)$, where ω is the angular THz frequency and φ is a phase acquired by a path length difference between source and receiver path. The laser beam

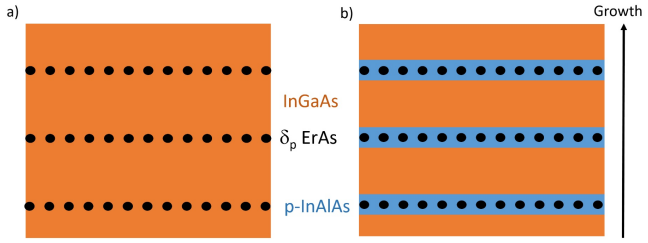

Fig. 2. a) typical cross section of an ErAs:InGaAs photoconductive receiver. The distance between the ErAs clusters along growth direction is 10 nm. The total thickness of the superlattice structure is 1 μm. b) a typical sample structure for ErAs:In(Al)GaAs sources. The InGaAs layers are 15 nm wide, the InAlAs layers are 3 nm wide (in total).

can be considered as a local oscillator that is mixed with the received THz field. Simply speaking, the mixing process generates a DC current that is $I_D \sim \cos\omega t \cos(\omega t + \varphi) = 0.5[\cos\varphi + \cos(2\omega t + \varphi)]$. The first term is a DC component that can be read out by post detection electronics, the second term is irrelevant for the detection process. A key problem at 1550 nm is designing a material that permits efficient operation at this long wavelength. For interband absorption, a band gap of about 0.8 eV is required, about a factor of 1.75 smaller than for 800 nm, where low temperature grown (LTG) GaAs is a well established photoconductive material. There are several challenges [12]: (i) a photoconductive detector requires high (illuminated) resistance, $R \sim 10$ kΩ, in order to limit thermal noise generated by the device. The thermal noise current is given by $I_N = \sqrt{4k_BT/R}$. The intrinsic carrier density, $n_i = \sqrt{N_V N_A}\exp[-E_G/(k_BT)]$, and thus the background conductivity even of undoped materials is exponentially higher with smaller band gap. As an example, for intrinsic GaAs, $n_i^{GaAs} = 2.1 \cdot 10^6/\text{cm}^3$ [13] while for $In_{0.53}Ga_{0.47}As$, a typical telecom material, it is more than five orders of magnitude higher with $n_i^{InGaAs} = 6.3 \cdot 10^{11}/\text{cm}^3$ [13]. A low carrier lifetime, τ_{rec}, may aid to reduce the free carrier density by trapping thermally activated carriers. (ii) It is further necessary to reduce the effect of the lifetime roll-off $\eta_{LT} = \left(1 + (2\pi\tau_{rec}f)^2\right)^{-1}$ [10], where f is the THz frequency. A particular problem for InGaAs is that most established traps, such as arsenic clusters by low temperature growth, ion-implanted material [14] or ErAs [12] is that the location of the trap states are close to the conduction band edge or even within the conduction band. Due to their fairly high density of states, the trap centers then increase the carrier concentration in the conduction band. Further, trapped carriers are quickly thermally reactivated, increasing the conductivity and the effective carrier lifetime. Most concepts therefore use heavy p-doping to push the Fermi level of the trap states closer to the band gap center. (iii) Last but not least, photoconductive detectors require high carrier mobility, μ, in order to generate a large detected current, $I_D \sim en_{opt}\mu E_{THz}$, where E_{THz} is the received THz field strength at the photoconductive gap and $n_{opt} \sim P_L(t)$ is the amount of carriers generated by the incident laser beam. Unfortunately, trapping centers

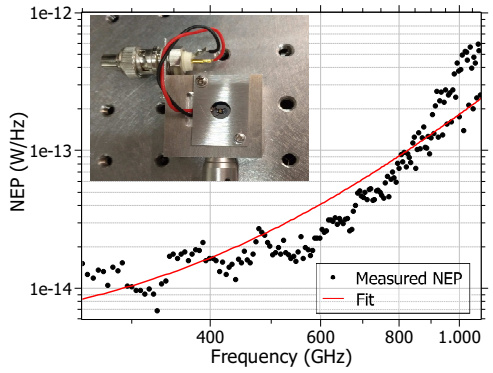

Fig. 3. NEP recorded with a Golay cell as reference power meter. The inset shows the device integrated with a silicon lens.

that are necessary for engineering the low lifetime are also excellent scattering centers, reducing the carrier mobility. Therefore, detector design requires a compromise between these aspects. We have recently shown that ErAs:In(Al)GaAs photoconductors are excellently suited for THz generation and detection in CW operation with a peak dynamic range of 78 dB and an (extrapolated) bandwidth of about 3.65 THz [12]. A cross section of the receiver material is illustrated in Fig. 2 a). The device consists of a superlattice of 10 nm $In_{0.53}Ga_{0.47}As$ and δp-doped 0.8 ML ErAs. The ErAs forms quasi-metallic precipitates that act as efficient recombination centers. Delta-p-doping around the ErAs layer improves the resistance of the device to values around 5-6 kΩ under illumination with 26 mW laser power. The dark resistance is orders of magnitude higher. The devices use two fingers at each electrode with a width of $w_E = 1.1$ μm and a spacing of the fingers of 1.9 μm. Fig. 3 shows the noise equivalent power of the device with 26 mW laser power. The THz power of a n-i-pn-i-p superlattice photomixer was focused by two TPX lenses on a Golay cell detector or the photoconductor, respectively. The Golay cell was recently calibrated to a Thomas Keating power meter. We allow for a power calibration error of 50% since Golay cell responsivities may vary with temperature, pressure or the way how the Golay cell is mounted in the system. The NEP is fairly flat up to about 500 GHz where the room temperature NEP is as low as 20$\pm$10 fW/Hz and increases towards higher frequencies. Also included in the graph is a fit with the calculated RC 3 dB frequency of 620 GHz, assuming a constant radiation resistance of the logarithmic spiral antenna of 70Ω while the capacitance was calculated from geometry, and a lifetime 3 dB frequency of 305 GHz due to the carrier lifetime of 0.52 ps obtained by optical pump-probe measurements. The amplitude is fitted. While the general agreement is fairly good, the measured graph remains flatter at frequencies below 500 GHz and shows a steeper increase at higher frequencies. Deviations from the calculated behavior may have several origins: (i) the capacitance of the finger structure is calculated using Eq. (1) from ref. [15] which is very accurate for a large amount of fingers, where fringing fields at the boundary of the structure play only a minor role. It may deviate for the structure used here. (ii) Another, potentially more relevant reason is alignment. Due to the diffraction limit and Airy effects by the finite size of the integrated silicon lens and the TPX lenses used in the setup, the position of the focal spot is slightly frequency-dependent, resulting in imperfect beam propagation at frequencies far away from the frequency where the system was aligned. For the shown measurement, the system was aligned at 500 GHz. (iii) the carrier lifetime is determined from pump-probe measurements [16]. Though this type of measurement is well established, it rather measures the carrier concentration, $n_{opt}(t)$ rather than the AC conductivity, $\sigma(t) = en_{opt}(t)\mu(t)$ which is relevant for the detection process. In particular, the carrier mobility will not be constant in the low field regime where the measurements take place [17].

IV. ErAs:In(Al)GaAs photoconductors, pulsed operation

ErAs:In(Al)GaAs photoconductors are also well suited for pulsed systems, both as source and receiver. Fig. 2 b) illustrates a typical source structure with a superlattice of 90 layers of 15 nm InGaAs, 1.5 nm p-InAlAs, 0.8 ML δp doped ErAs, 1.5 nm p-InAlAs. The largest bandwidth obtained so far is 6.5 THz [18] by using a 25 μm slotline with a sample structure as shown in Fig. 2 b) as source and a 25 μm H-dipole with a gap of 5 μm as receiver with a sample structure as shown in Fig. 2 a). Fig. 4 (top) shows a spectrum obtained with the same receiver as in ref. [18] and a 35 μm slotline as source, averaged over 2000 traces. The DC bias field strength is 60 kV/cm. The source laser power is 45 mW and the receiver laser power is 16 mW. The peak dynamic range at 600 GHz

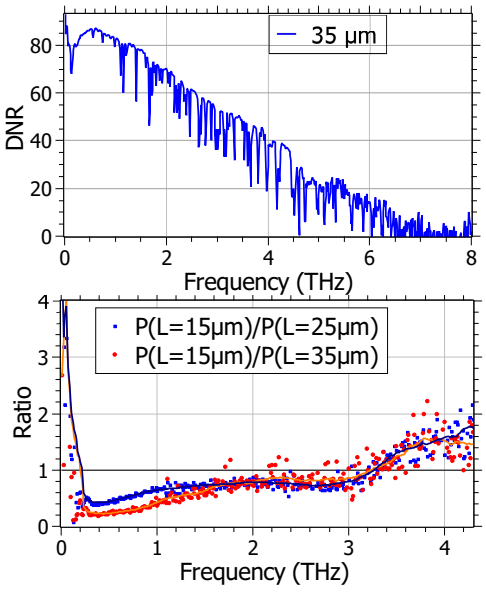

Fig. 4. a) Spectrum obtained with a 35 μm slotline as source and a 25 μm H-dipole as receiver. b) spectrum of a 15 μm slotline source, normalized to that of a 35 μm slotline source and a 25 μm slotline source. The solid lines are sliding averages for better visibility.

is 87 dB at these settings. At 4.1 THz, the system still offers 40 dB. The bandwidth is greater than 6 THz. Fig. 4 (bottom) shows the comparison of the output power of a 15 μm slotline normalized to that of the 35 μm slotline or a 25 μm slotline.

While the 35 μm (25 μm) antenna shows 6 dB (3 dB) higher output around the peak frequency of 600 GHz, the 15 μm antenna shows slightly improved bandwidth and about 2.4 dB (1.8 dB) higher dynamic range beyond 4 THz. The antenna length can therefore be used for fine-tuning the emission spectra.

V. Conclusion and Outlook

We have shown three examples of high performance materials for THz applications that use ErAs quasi-metallic inclusions. In all three cases, the ErAs precipitates act as efficient recombination centers for free carriers. For continuous-wave photomixing, the n-i-pn-i-p superlattice concept employs ErAs within a highly doped np junction as low resistance recombination diode between two subsequent p-i-n diode THz sources, connected in series, reaching about 1μW of power at 500 GHz with only 4 mA photocurrent. The current main limitation is poor optical coupling by vertical illumination. Waveguide-integration will increase the absorption by 5-7 times. In terms of photoconductive materials, the ErAs precipitates are implemented as carrier trapping centers, lowering the carrier lifetime to 0.52 ps. Continuous-wave receivers show a NEP of 20$\pm$10 pW/Hz at 0.5 THz. In pulsed systems, ErAs:In(Al)GaAs devices are employed as both source and receiver. We have compared different antenna designs for optimization of bandwidth at the cost of dynamic range at the peak value.

Acknowledgment

We thank D. Cibiraite, A. Lisauskas, and H. Roskos from Johann Wolfgang Goethe-Universität, Frankfurt(Main), Germany, for help with the calibration of the Golay cell. We acknowledge funding by the Deutsche Forschungsgemeinschaft, Project PR1413/3-1 (REPHCON) and from the European Research Council (ERC) under the European Union's Horizon 2020 research and innovation programme (grant agreement No. 713780) and the CST AG for providing the CST Studio Suite.

References

[1] T. Göbel, D. Stanze, B. Globisch, R. J. B. Dietz, H. Roehle, and M. Schell, "Telecom technology based continuous wave terahertz photomixing system with 105 decibel signal-to-noise ratio and 3.5 terahertz bandwidth," Opt. Lett., vol. 38, pp. 4197-4199, 2013.

[2] R. Piesiewicz, C. Jansen, S. Wietzke, D. Mittleman, M. Koch, and T. Kürner, "Properties of building and plastic materials in the Thz range," Int J Infrared Milli Terahz Waves, vol. 28, p. 363, 2007.

[3] V. Rymanov, A. Stöhr, S. Dülme, and T. Tekin, "Triple transit region photodiodes (TTR-PDs) providing high millimeter wave output power," Optics Express, vol. 22, p. 7550, 2014.

[4] K. Sun, D. Jung, C. Shang, A. Liu, J. Bowers and A. Beling, "Low-dark current III-V photodiodes grown on silicon substrate," 2017 IEEE Photonics Conference (IPC), Orlando, FL, pp. 95-96, 2017.

[5] A. J. Seeds, H. Shams, M. J. Fice, and C. C. Renaud, "Terahertz photonics for wireless communications," J. Lightwave Technol. vol. 33, pp. 579-587, 2015.

[6] R. Chuenchom et al., "Integrated 110 GHz coherent photonic mixer for CRoF mobile backhaul links," 2015 International Topical Meeting on Microwave Photonics (MWP), pp. 1-4, 2015.

[7] T. Nagatsuma, K. Kato, and J. Hesler, "Enabling technologies for real-time 50-Gbit/s wireless transmission at 300 GHz." Proceedings of the Second Annual International Conference on Nanoscale Computing and Communication. ACM, p.10, 2015.

[8] G. H. Döhler et al., "THz-photomixer based on quasi-ballistic transport". Semiconductor Sci. and Technol, vol. 20, p. 178-190, 2005.

[9] S. Preu, F. H. Renner, S. Malzer, G. H. Döhler, M. Hanson, A. C. Gossard, T. L. J. Wilkinson, E. R. Brown, and L. J. Wang, "Efficient terahertz emission from ballistic transport enhanced n-i-p-n-i-p superlattice photomixers", Appl. Phys. Lett., vol. 90, 212115, 2007.

[10] S. Preu, G. H. Döhler, S. Malzer, A. C. Gossard, and L. J. Wang, "Tunable, Continuous-Wave Photomixer Sources and Applications," J. Appl. Phys. vol. 109, 061301, 2011.

[11] C.C. Renaud, M. Natrella, C. Graham, J. Seddon, F. Van Dijk, and A.J. Seeds, "Antenna Integrated THz Uni-Traveling Carrier Photodiodes," IEEE J. Sel. Topics in Quantum Electron., vol. 24, pp. 1-11, 2018.

[12] A.D.J. Fernandez Olvera, H. Lu, A.C. Gossard, and S. Preu, "Continuous-wave 1550 nm operated terahertz system using ErAs:In(Al)GaAs photo-conductors with 52 dB dynamic range at 1 THz," Optics Express, vol. 25, pp. 29492-29500, 2017.

[13] http://www.ioffe.ru/SVA/

[14] J. Mangeney, "THz photoconductive antennas made from ion-bombarded semiconductors," J. of Infrared, Millim. and Terahz Waves vol. 33, p. 455, 2012.

[15] E.R. Brown, "THz generation by photomixing in ultrafast photoconductors," Int. J. of High Speed Electronics and Systems, vol. 13, pp. 497-545, 2003.

[16] J. Y. Suen, P. R. Krogen, S. Preu, H. Lu, A. C. Gossard, D. C. Driscoll, and P. M. Lubin, "Measurement and modeling of ErAs:$In_{0.53}Ga_{0.47}As$ nanocomposite photoconductivity for THz generation at 1.55 μm pump wavelength" J. of Appl. Phys. vol. 116, 013703, 2014.

[17] Z. Jin, D. Gehrig, C. Dyer-Smith, E. J. Heilweil, F. Laquai, M. Bonn, and D. Turchinovich, "Ultrafast Terahertz photoconductivity of photovoltaic polymer-fullerene blends: a comparative study correlated with photovoltaic device performance," J. of Phys. Chem. Lett. vol. 5, pp. 3662-3668, 2014.

[18] U. Nandi, J. C. Norman, A. C. Gossard, H. Lu, and S. Preu, "1550-nm driven ErAs:In(Al)GaAs photoconductor-based terahertz time domain system with 6.5 THz bandwidth," J. of Infrared, Millim. and Terahz Waves, vol. 39, pp. 340-348, 2018.

Published article: M. Mendez Aller, et al. *ErAs Enhanced Active Photonic THz Components.* In: 2018 First International Workshop on Mobile Terahertz Systems (IWMTS). IEEE, 2018. p. 1-4. DOI: 10.1109/IWMTS.2018.8454690